

Contribution of nano-copper particles to *in vivo* liver dysfunction and cellular damage: Role of I κ B α /NF- κ B, MAPKs and mitochondrial signal

Prasenjit Manna, Manoranjan Ghosh, Jyotirmoy Ghosh, Joydeep Das & Parames C. Sil

To cite this article: Prasenjit Manna, Manoranjan Ghosh, Jyotirmoy Ghosh, Joydeep Das & Parames C. Sil (2012) Contribution of nano-copper particles to *in vivo* liver dysfunction and cellular damage: Role of I κ B α /NF- κ B, MAPKs and mitochondrial signal, Nanotoxicology, 6:1, 1-21, DOI: [10.3109/17435390.2011.552124](https://doi.org/10.3109/17435390.2011.552124)

To link to this article: <https://doi.org/10.3109/17435390.2011.552124>




View supplementary material 



Published online: 14 Feb 2011.



Submit your article to this journal 



Article views: 275



Citing articles: 29 View citing articles 

Contribution of nano-copper particles to *in vivo* liver dysfunction and cellular damage: Role of I κ B α /NF- κ B, MAPKs and mitochondrial signal

PRASENJIT MANNA, MANORANJAN GHOSH, JYOTIRMOY GHOSH, JOYDEEP DAS, & PARAMES C. SIL

Division of Molecular Medicine, Bose Institute, Calcutta, West Bengal, India

(Received 13 April 2010; accepted 3 January 2011)

Abstract

The present study investigated the oxidative stress responsive cell signaling in nano-copper-induced hepatic dysfunction and cell death. Exposure to nano-copper (18 nm) dose-dependently (200–600 mg/kg bw) reduced the hepatic index, caused oxidative stress and led to hepatic dysfunction. Nano-copper burden also increased the transcriptional activity of NF- κ B, up-regulated the expression of phosphorylated p38, ERK1/2 and caused the reciprocal regulation of Bcl-2 family proteins, disruption of mitochondrial membrane potential, release of cytochrome C, formation of apoptosome and activation of caspase 3. DAPI staining, immunofluorescence study, FACS analysis and histological findings also support this observation. Soluble copper (Cu⁺², 110 mg/kg bw)-exposed animals were used as a positive control. Different doses of particulate and soluble forms were used in the study because of different LD₅₀ values. The results suggest that nano-copper induces hepatic dysfunction and cell death via the oxidative stress-dependent signaling cascades and mitochondrial event.

Keywords: *Nano-copper particles, hepatic dysfunction, antioxidant defense I κ B α /NF- κ B, MAPKs, Bcl-2 family proteins, mitochondrial signal and apoptosis of hepatocytes*

Introduction

In the last decade, new directions of modern research broadly defined as ‘nanoscale science and technology’ have emerged. Nanotechnology involves the creation and manipulation of materials at nanoscale levels (1–100 nm). Nanomaterials have unique physico-chemical properties (like ultra small size, large surface area to mass ratio and extremely high chemical reactivity) which make them different from bulk materials of the same composition (Oberdörster et al. 2005, 2007). These properties can be used to overcome some of the limitations found in traditional therapeutic and diagnostic agents. The application of nanotechnology to medicine, known as nanomedicine, concerns the use of nanomaterials to develop novel therapeutic and diagnostic tool (Zhang et al. 2007). The difference between nanomedicine and conventional drugs is that nanomedicine is entirely based on small molecule chemistry. They not only act as therapeutic agents but also deliver themselves to specific regions or tissues in the body (Kipen and Laskin 2005). While benefits of nanotechnology are

widely expected, however both academic and public concerns begin to emerge on the potentially adverse effects of these manufactured nanomaterials. Thus, nanotoxicology is emerging as an important sub-discipline of nanotechnology. Exposure to nano-structures occurs in a variety of manners, such as researchers of the manufacturing nanoparticles, patients injected with nanostructures, or people using products containing nanostructures. After exposure and absorption, they enter into the cells of different organs, interact with the macromolecules like protein, DNA etc., and cause organ pathophysiology.

The transition metal copper is a well known essential trace element. It functions as a catalytic co-factor in a number of redox enzymes needed in a wide range of metabolic processes (Georgopoulos et al. 2001). The biological functions of copper include electron-transfer catalysis by means of its two accessible oxidation states. Copper deficiency, on the other hand, leads to several diseases in human. When the intake of copper exceeds the range of human tolerance (commonly known as copper overload), the metal would exert toxic effects, causing jaundice, hemolysis etc.,

Correspondence: Parames C. Sil, PhD, Professor, Division of Molecular Medicine, Bose Institute, P-1/12, CIT Scheme VIIM, Calcutta-700054, West Bengal, India. Tel: +91 33 2569 3243. Fax: +91 33 2350 6790. E-mail: parames@bosemain.boseinst.ac.in

(Bjorn et al. 2003) and cell death (Nawaz et al. 2006). The excessive copper can promote damage to cellular molecules and alter their structures via the formation of free radicals (Ozcelik et al. 2003). Recent studies indicate that *in vivo* copper overload induces a set of toxicological activities such as oxidative stress, changes in lipid profile, renal dysfunction and hepato-cirrhosis etc. Nano-sized copper particles are now industrially produced and they are commercially available. Recently, nano-copper particles are used as the additive in lubricants, polymers/plastics, metallic coating and inks, etc. Due to excellent mending effects, nano-copper particles are added into lubricant oil to effectively reduce friction and are also used to mend a worn surface (Liu et al. 2004). Nano-copper particles are homogeneously deposited on the surface of graphite to improve the charge/discharge property, such as coulombic efficiency, cycle characteristic etc. (Guo et al. 2002). The nano-sized copper-fluoro polymer is employed as bioactive coatings that are capable of inhibiting the growth of microorganisms (Cioffi et al. 2005). These nanomaterials are likely to enter the environment and human body via different paths such as effluent, spillage during shipping and handling, consumer products and disposal, etc.

Earlier studies suggest that nano-sized copper particles are more toxic than the micro-copper and copper ion (Chen et al. 2006). Exposure to nano-copper particles caused alteration in the serum marker enzymes related to different organ (liver, kidney, etc.) pathophysiology (Chen et al. 2006). No report has, however, been found so far in the literature describing the role of oxidative stress responsive signaling cascades in copper nanoparticles-induced liver toxicity and cell death. In our present study, we investigated the status of the intracellular antioxidant defense machineries and the oxidative stress responsive cell signaling cascades in nano-copper particles-induced hepatic dysfunction and hepatocytes cell death.

Materials and methods

Chemicals

Rhodamines 123, anti Cytochrome C, anti Caspase-3, anti Cleaved Caspase-3, anti Apaf1, anti ERK 1/2 and anti phosphorylated ERK1/2 antibodies were purchased from Sigma-Aldrich Chemical Company (St Louis, MO, USA). Anti NF- κ B (p65 sub unit), anti phosphorylated NF- κ B (p65 sub unit), anti Bcl-2, anti Bad, anti p38 and anti phosphorylated p38 antibodies were purchased from Cell signaling technology (Beverly, MA, USA). All other antibodies were purchased from Santa Cruz Biotechnology (Santa

Cruz, USA). Other chemicals and reagents were of the highest analytical grade and were bought from Sisco Research Laboratory (Mumbai, India).

Animals

Swiss albino male mice, weighing approximately 20–22 g were acclimatized under laboratory condition for two weeks prior to the experiments. They were maintained under standard conditions of temperature ($23 \pm 2^\circ\text{C}$) and humidity ($50 \pm 10\%$) with an alternating 12 h light/dark cycles. All the experiments with animals were carried out according to the guidelines of the institutional animal ethical committee.

Preparation of nano-copper (Cu) particles

Copper (Cu) nanoparticles were prepared following the method of Zhu et al. (2005). Briefly, 20 ml solution of $\text{CuSO}_4 \cdot 5\text{H}_2\text{O}$ in ethylene glycol (EG) was mixed with 20 ml solution of NaOH and N_2H_4 , H_2O in EG under magnetic stirring. The molar ratio of N_2H_4 , $\text{H}_2\text{O}/\text{CuSO}_4 \cdot 5\text{H}_2\text{O}$ was 1.5 and the molar ratio of NaOH/ $\text{CuSO}_4 \cdot 5\text{H}_2\text{O}$ was 0.05. The mixed solution was placed in a microwave oven (2.45 GHz) and allowed to react under medium power (750 W) for 3 min. Upon irradiating for about 30 s, the mixture turned black from light blue; at about 90 s, the mixture started boiling at about 196°C . It was then irradiated for another 2 min to keep the mixture boiling. After cooling to room temperature, Cu nanoparticles were obtained as precipitate by centrifugation and that was washed with ethanol for several times. Transmission electron microscope (TEM, JEOL JEM-2010), Dynamic Light Scattering (DLS, Nano-S, Malvern, UK) and Energy Dispersive X-ray spectroscopy (EDX, FEI Quanta 200) were used to characterize (morphology, size distribution and identity) the synthesized copper nanoparticles.

Animal treatment

The animals were divided into five groups each consisted of six mice and they were treated as follows. Group 1 animals received only normal diet and served as control group. Animals of the subsequent groups, group 2 (Cu-1), group 3 (Cu-2), group 4 (Cu-3) received Cu nanoparticles via oral gavages at a dose of 200, 413 and 600 mg/kg body weight, respectively, for three days. Group 4 animals received copper chloride at a dose of 110 mg/kg body weight for three days and served as copper ion group (Cu^{+2}). The dose schedules of Cu nanoparticles and copper ion have been selected based on the earlier reports of Chen et al. (2007).

After three days of treatment, the animals were euthanized and blood samples were collected in tubes containing a mixture of potassium oxalate and sodium fluoride (1:3) for the estimation of serum parameters related to liver dysfunction. From all the sacrificed animals the liver tissue were collected, weighed, stored at 4°C and used for the experiments as needed in the present study.

Preparation of liver tissue homogenates

About 200 mg liver tissue was homogenized using glass homogenizer in 100 mM phosphate buffer (pH 7.4), containing 1 mM EDTA, PMSF (proteinase inhibitor, 1 mM) as well as phosphatase inhibitor cocktail (1:100 dilution) and the mixture was centrifuged at 12,000 *g* for 30 min at 4°C. The supernatant was collected and used for the experiments.

Isolation of hepatocytes from liver tissue of in vivo experimental animals

Hepatocytes were isolated from liver tissue of *in vivo* experimental animals by the perfusion technique as described by Ghosh and Sil (2009). After sacrifice of the *in vivo* experimental animals, liver tissues were collected. Then the organs were extensively perfused *in situ* in phosphate buffer saline to get rid of blood and irrigated in a buffer containing Hepes (10 mM), KCl (3 mM), NaCl (130 mM), NaH₂PO₄-H₂O (1 mM) and glucose (10 mM) pH 7.4. The livers were then incubated with a second buffer containing CaCl₂ (5 mM), 0.05% collagenase type I mixed with the buffer previously described for about 45 min at 37°C. The solution was then passed through wide bore syringe, filtered, centrifuged and the pellet was suspended in DMEM containing 10% FBS and the suspension was adjusted to obtain $\sim 2 \times 10^6$ cells/ml. Only the preparations with cell viability (measured by MTT assay) greater than 90% were used for subsequent experiments.

Determination of protein content

The protein contents of the liver tissue homogenates of the experimental animals were measured by the method of Bradford using crystalline BSA as standard (Bradford 1976).

Assessment of the levels of serum specific markers related to hepatic dysfunction

Blood samples collected from puncturing mice hearts were kept overnight to clot and then centrifuged at 3,000 *g* for 10 min. Serum-specific markers

(alanine transaminase [ALT] and alkaline phosphatase [ALP]), related to hepatic dysfunction, were measured by using kits (Span Diagnostic Ltd, India).

Measurement of intracellular ROS production and serum NO (nitrate-nitrite) levels

Intracellular ROS production was estimated by using 2,7-dichlorofluorescein diacetate (DCFDA) as a probe using the method of LeBel and Bondy (1990) followed by the modification introduced by Kim et al. (1996). Briefly, 100 µl of tissue homogenates were incubated with the assay media (20 mM tris-HCl, 130 mM KCl, 5 mM MgCl₂, 20 mM NaH₂PO₄, 30 mM glucose and 5 µM DCFDA) at 37°C for 15 min. The formation of DCF was measured at the excitation wavelength of 488 nm and emission wavelength of 610 nm for 10 min by using a fluorescence spectrometer (Hitachi, Model No F4500) equipped with a FITC filter.

For *in vitro* study, after treatment, the medium was aspirated and hepatocytes were washed with RPMI 1640 culture medium and incubated in 2 ml of fresh culture medium without FBS. DCFDA was added at a final concentration of 10 µmol/l and incubated for 20 min. The cells were then washed twice with RPMI 1640 culture medium and maintained in 1 ml same medium. Fluorescence was monitored using a fluorescence spectrometer and they were also assessed using a flow cytometer (Becton Dickinson, Mountain View, CA, USA).

The levels of serum NO have been measured by estimating the concentration of nitrate and nitrite with a modified nitrate reductase and Griess reaction method (Hevel and Marietta 1994). Nitrate was reduced to nitrite by the action of nitrate-reductase in the presence of NADPH. Excess NADPH was then consumed and the nitrite concentration was measured by the addition of equal volumes of 1% sulfanilamide in 5% concentrated phosphoric acid and 0.1% N-(1-naphthyl) ethylene diamine dihydrochloride. The Griess color reaction forms a pink azo dye with an absorbance wavelength of 540 nm. The assay was standardized using various dilutions of sodium nitrate and nitrite (Sigma-Aldrich Chemical Company, S. Louis, MO, USA).

Assay of biochemical parameters including antioxidant enzymes, GSH/GSSG, lipid peroxidation and protein carbonylation

Oxidative stress has been suggested to play an important role in nano-copper-induced organ disorders. To protect against oxidative stress, cells usually possess defensive mechanisms with the help of its own

intracellular antioxidants (like antioxidant enzymes and cellular metabolites). In our study we, therefore, investigated the activities of the antioxidant enzymes (SOD, CAT, GST, GR and GPx), GSH/GSSH ratio, levels of the lipid peroxidation and protein carbonylation in the experimental animals following the methods as mentioned elsewhere (Manna et al. 2009).

Immunoblotting

Samples containing 50 µg proteins were subjected to 10% SDS-PAGES and transferred to a nitrocellulose membrane. Membranes were blocked at room temperature for 2 h in blocking buffer containing 5% non-fat dry milk to prevent non-specific binding and then incubated with primary antibodies overnight at 4°C. The primary antibodies used in the present study were anti-p38 (1:1000), anti-phosphorylated p38 (1:1000 dilution), anti-ERK1/2 (1:1000), anti-phosphorylated ERK1/2 (1:1000), anti-NF-κB (p65) (1:250 dilution), anti-phosphorylated NF-κB (p65) (1:500), anti-IκB-α (1:1000 anti-phosphorylated IκB-α (1:500), anti-complex II (1:1000), anti-cytochrome C (1:1000), anti-caspase 3 (1:1000), anti-cleaved caspase 3 (1:1000), anti-caspase 9 (1:1000) and anti-Apaf1 (1:1000) antibodies. The membranes were washed in TBST (50 mmol/l Tris-HCl, pH 7.6, 150 mmol/L NaCl, 0.1% Tween 20) for 30 min and incubated with appropriate HRP conjugated secondary antibody (1:2000) for 2 h at room temperature and developed by the HRP substrate 3,3'-Diaminobenzidine tetrahydrochloride (DAB) system (Bangalore, India).

Preparation of nuclear extract from liver tissue

Nuclear proteins were extracted from the frozen liver samples according to the method of Valen et al. (2000). Briefly, livers were homogenized and lysis buffer was added. After incubation on ice, nuclei were collected by means of centrifugation for 1 min at 8000 *g*. The pellet was washed with 20 mM KCl buffer, centrifuged again, and resuspended in 20 mM KCl buffer. An equal part 600 mM KCl was added to the pellet and kept on ice for 30 min. After centrifugation for 15 min at 8000 *g*, the supernatant containing nuclear proteins was obtained. This nuclear extract was subjected to immunoblotting as described above to determine the activity of NF-κB *in vivo*.

Isolation of mitochondria and determination of mitochondrial membrane potential ($\Delta\psi_m$)

Mitochondria were isolated from the liver tissue of experimental animals. Briefly, the liver tissue

homogenate was overlaid on 0.75 M sucrose in HEPES buffer and centrifuged for 30 min at 10,000 *g*. The supernatant was discarded and the mitochondria pellet were re-suspended in HEPES buffer and recentrifuged for 10 min at 10,000 *g*. This supernatant was also discarded and the final mitochondrial pellet was re-suspended in PBS. It was stored at -80°C until use. The purity of mitochondrial fraction was checked by immunoblotting analysis with anti-complex II antibody. Analytic flow cytometric measurements for the membrane potential ($\Delta\psi_m$) of isolated mitochondria were performed using FACScan flow cytometer (Becton Dickinson, Mountain View, CA, USA) equipped with an argon laser excitation at 488 nm and 525 nm band pass filter (Bai et al. 1999). Mitochondrial membrane potential ($\Delta\psi_m$) was estimated on the basis of cell retention of the fluorescent cationic probe rhodamine 123 (5 µg/ml final concentration).

Assay of cytochrome C in the cytosolic and mitochondrial fraction

Depletion in mitochondrial membrane potential causes the release of cytochrome C and initiates mitochondrial-dependent cell death pathway. Concentration of cytosolic cytochrome C was measured with the cytochrome C enzyme immunometric assay kit (Minneapolis, USA). The expression of mitochondrial cytochrome C was investigated by immunoblotting analysis using anti-cytochrome C antibody.

HPLC measurement of 8-hydroxy-2-deoxyguanosine (8-OHdG) and 2-deoxyguanosine (2-dG)

DNA samples were isolated from the experimental liver tissue using standard kit. The isolated DNA samples were digested following the method of Kasai et al. (1986). The oxidative DNA adducts, 8-OHdG was measured with HPLC equipped with electrochemical and UV detection following the methods as described elsewhere (Kasai et al. 1986). The wavelength for UV detection of 2-dG was set at 260 nm. The mobile phase was composed of 50 mM sodium acetate, 5% methanol; pH 5.2 and flow rate was 1.0 ml/min.

Flow cytometric analysis

The flow cytometric analysis was performed using FACS Calibur (Becton Dickinson, Mountain View, CA, USA) equipped with 488 nm argon laser light source. Cell debris, characterized by a low FSC/SSC was excluded from analysis. The data

was analyzed by Cell Quest software (BD Biosciences, CA, USA).

Assessment of apoptotic and necrotic cells

The apoptotic and necrotic cell distribution was analyzed by Annexin V binding and PI uptake. Positioning of quadrants on Annexin V/PI dot plots was performed and living cells (Annexin V⁻/PI⁻), early apoptotic/primary apoptotic cells (Annexin V⁺/PI⁻), late apoptotic/secondary apoptotic cells (Annexin V⁺/PI⁺) and necrotic cells (Annexin V⁻/PI⁺) were distinguished. Therefore, the total apoptotic proportion included the percentage of cells with fluorescence Annexin V⁺/PI⁻ and Annexin V⁺/PI⁺. The cells were suspended in 1 ml binding buffer (1×). An aliquot of 100 µl was incubated with 5 µl Annexin V-FITC and 10 µl PI for 15 min in dark at room temperature and 400 µl binding buffer (1×) was added to each sample. The FITC and PI fluorescence were measured through FL-1 filter (530 nm) and FL-2 filter (585 nm), respectively, and 10,000 events were acquired.

Histological studies

Livers from all the experimental animals were fixed in 10% buffered formalin and were processed for paraffin sectioning. Sections of about 5 µm thickness were stained with haematoxylin and eosin to evaluate the pathophysiological changes under light microscope.

Immunohistochemistry

Immunohistochemical staining was performed to detect expression of cleaved caspase-3. The sections were at first deparaffinized with xylene and then dehydrated with 100%, 98%, and 70% ethanol accordingly. Endogenous peroxidase was blocked by immersing slides in methanol with 0.3% hydrogen peroxide for 30 min. Next, the sections were incubated in 5% skim milk for 30 min at room temperature. The antibody-binding epitope of the antigen was retrieved by microwave treatment for 30 min in boiling 10 mM citrate buffer (pH 6.0). The slides were allowed to cool for 20 min in the citrate buffer before further treatment. After a quick rinse in phosphate buffered saline, the sections were incubated overnight at 4°C with the anti-cleaved caspase 3 antibody (1:50 dilution). After washing, the sections were overlaid with peroxidase-conjugated secondary antibody for 1 h. The chromogenic reaction was developed with diaminobenzidine solution. After chromogenic staining, the sections were counterstained with hematoxylin solution for

1 min (caused dark blue/black spot) and then thoroughly rinsed with the distilled water. The entire procedure developed dark blue or black spot with pinkish-blue background for the increased expression of Capase 3.

In vitro experiment on isolated hepatocytes from control animal

Hepatocytes were isolated from liver tissue of control animals by the perfusion technique as described earlier Ghosh and Sil (2009). After isolation, hepatocytes were treated with nano-copper (50 µM) in a time-dependent manner (for SOD and CAT assay the time periods were 15, 30 and 60 min; for the NF-κB assay the time periods were 1, 2, 4 and 6 h). After incubation, hepatocytes were harvested for further time-dependent immunoblotting analyses.

Statistical analysis

All the values are expressed as mean ± SD ($n = 6$). Significant differences between the groups were determined with SPSS 10.0 software (SPSS Inc., Chicago, IL, USA) for Windows using one-way analysis of variance (ANOVA) and the group means were compared by Student-Newman-Keuls post-hoc tests. A difference was considered significant at the $p < 0.05$ level.

Results

Nanoparticle characterizations

The sizes of the copper nanoparticles were determined by Transmission Electron Microscope (TEM), (Figure 1A). The TEM image showed that average size of nano-copper particles is 18 nm in diameter. The size distribution and the polydispersity index (PDI) were also determined by a Dynamic Light Scattering (DLS) experiment (Figure 1B). The PDI value has been found to be 0.514 and a single peak appeared around 18.62 nm (diameter) with 100% intensity support the TEM image as well as uniformity of the size distribution. Finally the identities of the copper nanoparticles were established by Energy Dispersive X-ray spectroscopy (EDX) (Figure 1C). Appearance of a large peak of copper in EDX spectroscopy also supports the identity of the copper particles.

Effects on hepatic dysfunction

Reduction in hepatic index and increased activities of membrane leakage serum marker enzymes, ALT and

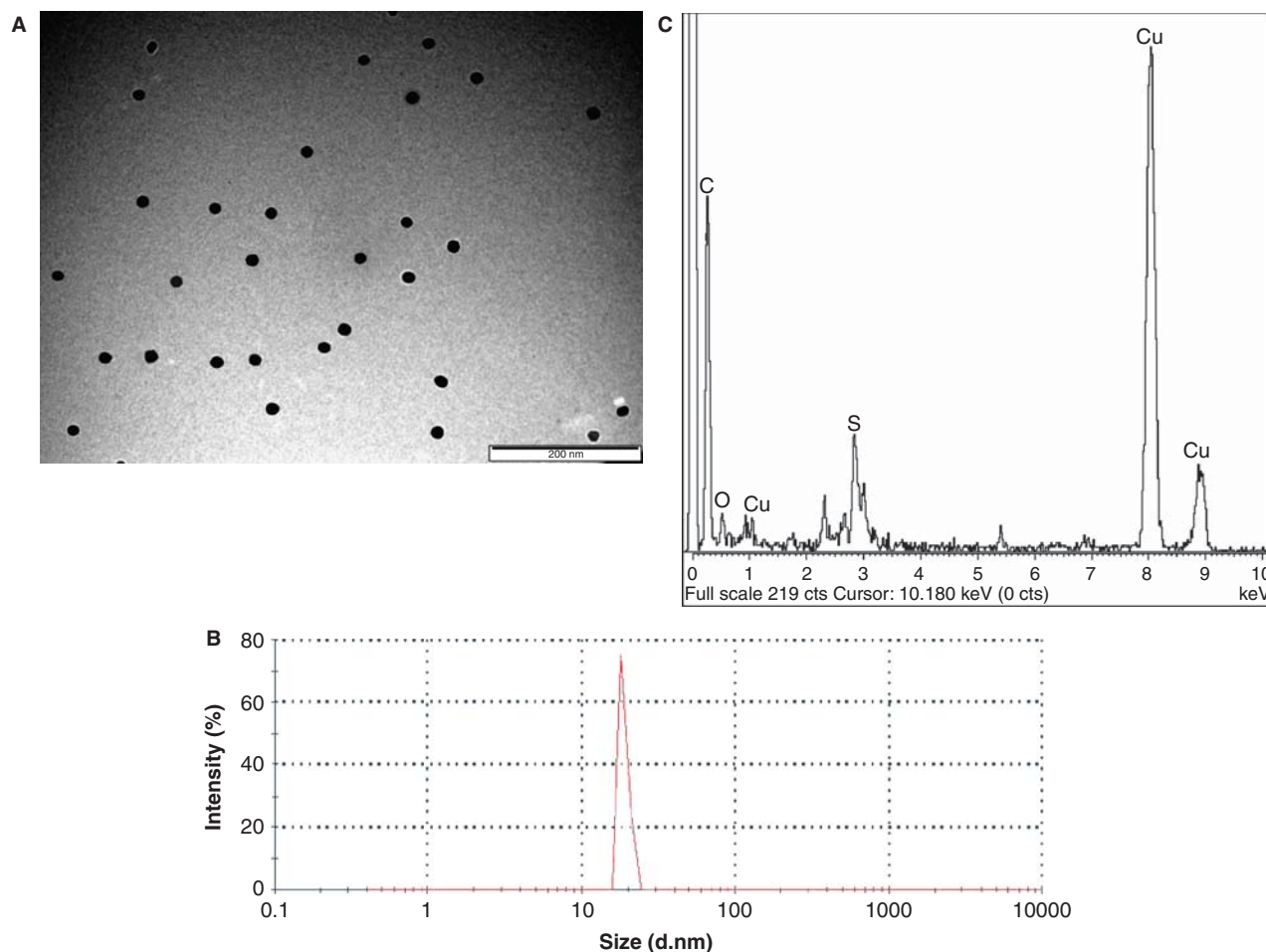


Figure 1. (A) TEM image of nano-copper particles. The scale bar used here is 200 nm. The average size of the particle is 18 nm. (B) Size distribution image of nano-copper particles obtained from DLS experiment. Peak indicates the particles with 18.62 nm in diameter with 100% intensity. PDI value is 0.514. (C) EDX spectroscopy of nano-copper particles.

ALP, are the markers for the development of hepatic dysfunction. Hepatic index (H_x) is defined as:

$$(H_x) = \frac{\text{weight of experimental liver/weight of the experimental animal}}{\text{weight of the control liver/weight of the control animal}}$$

Exposure to drugs and harmful chemicals reduces the liver weight to body weight ratio which in turn causes reduction in hepatic index. ALT and ALP are two well-known membrane bound enzymes related to hepatic dysfunction. During hepatic injury, the cell membrane is disrupted and these enzymes come out into the blood stream. As a result their concentrations are elevated. The levels of these enzymes along with the hepatic index clearly speak about the hepatic physiology. It has been observed that administration with nano-copper particles dose-dependently reduced the hepatic index and simultaneously increased the activities of ALT and ALP (Figure 2) suggesting the hepatic dysfunction.

Effects on intracellular ROS and NO production

Several investigations support the fact that increased production of ROS as well as RNS play an important role in copper-induced organ dysfunction. Exposure to nano-sized copper particles caused alteration in the levels of intracellular ROS as well as NO production (measured by nitrite level) (Figure 3, Panel A). Increased production of ROS was also monitored using fluorescence microscope and flow cytometer. Under fluorescence microscope, an increased number of green fluorescent cells represents the increased production of intracellular ROS. In flow cytometric analysis, it has also been observed that dose-dependent exposure of nano-copper increased the percentage of FL-1 binding compared to control, indicating the increased number of cells with DCF fluorescence (Figure 3, Panel B). In all these experiments, we observed that nano-copper at a dose of

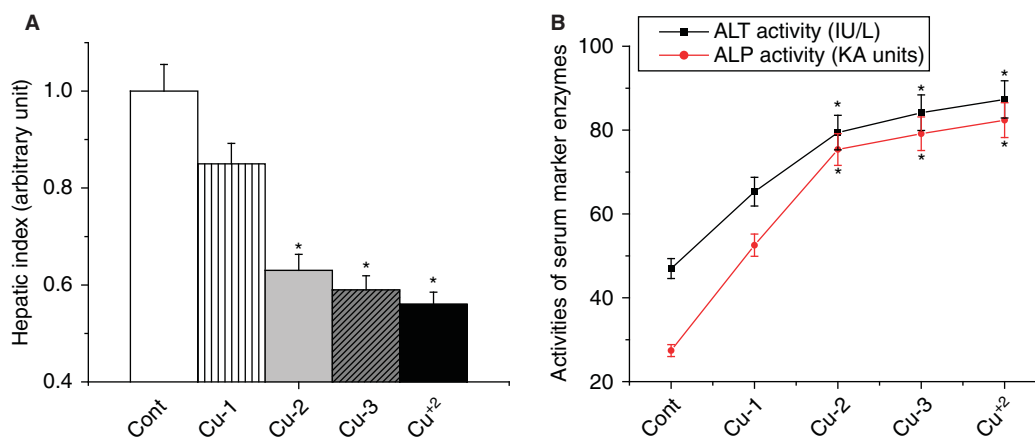


Figure 2. Dose-dependent effect of nano-copper particles on the reduction of hepatic index (Panel A) as well as increased activities of the serum marker enzymes, ALT and ALP, (Panel B) related to hepatic dysfunction. Cont: control mice, Cu-1, Cu-2 and Cu-3: animals administered with nano-copper particles at a dose of 200, 413 and 600 mg/kg body weight. Data are mean \pm SD, for six animals per group and were analyzed by one-way ANOVA, with Student-Newman-Keuls post-hoc tests. Significant differences (*) were attributed at $p < 0.05$.

413 mg/kg body weight or above caused significant production of reactive intermediates. The large surface area and the high reactivity make these nanomaterials potential inducers of the production of reactive intermediates.

Estimation of lipid peroxidation and protein carbonyl content

Lipid peroxidation and protein carbonyl content are widely used as the marker of cell membrane damage and oxidative modification of proteins. In the present study, the lipid peroxidation has been measured by estimating the concentration of MDA (lipid peroxidation end product). Exposure with nano-copper particles increased the levels of MDA and protein carbonylation in the liver tissue of the experimental animals (Figure 4).

Effects on GSH/GSSG and 8-OHdG/2-dG ratios

GSH plays an important role in scavenging intracellular reactive intermediates. A massive amount of GSH is consumed to accomplish this task. Whenever the GSH level decreases below the threshold level, the concentration of reactive intermediates gets elevated and cause oxidative stress as well as DNA damage. In our study, we found that intracellular copper overload decreased the GSH/GSSG ratio with simultaneous increase in DNA oxidation (as measured by 8-OHdG/2-dG ratio) (Figure 4).

Activities of hepatic antioxidant enzymes

Oxidative stress is the result of a redox imbalance between the generation of ROS and the compensatory

response from the endogenous antioxidant network. To investigate the status of the intracellular antioxidant defense machineries, we measured the activities of antioxidant enzymes, SOD, CAT, GST, GR and GPx. Figure 5 (Panel A) represents the activities of the antioxidant enzymes in liver tissue of the experimental animals. Our study reveals that nano-copper administration dose-dependently attenuated the activities of the antioxidant enzymes. In line with the biochemical assays, immunoblotting analyses (Figure 5, Panel B) with anti SOD and anti CAT antibodies, revealed that nano-copper exposure also reduced the expressions of those antioxidant enzymes in a dose-dependent manner.

In the present study, the dose-dependent toxicity of nano-copper was compared with a copper ion-treated group (Figure 5). It has been observed that copper ion (Cu^{+2}) exposure significantly reduced the hepatic index (Figure 2A) and increased release of membrane bound enzymes related to hepatic dysfunction (ALT, ALP) (Figure 2B) as well as the oxidative stress markers (e.g., ROS as well as NO production, lipid peroxidation, protein carbonylation, GSH/GSSG, antioxidant enzymes etc.) (Figures 3–5). We found that toxicity of nano-copper at a dose of 413 mg/kg body weight or above is similar to those of copper ion at a dose of 110 mg/kg body weight. Literature (Chen et al. 2006) suggests that in the stomach, nano-copper particles are rapidly converted to copper ions which can easily enter into the cell causing intracellular copper overload. Thus, nano-copper-induced oxidative organ dysfunction is mostly due to their rapid conversion into the copper ion and increasing cellular copper burden.

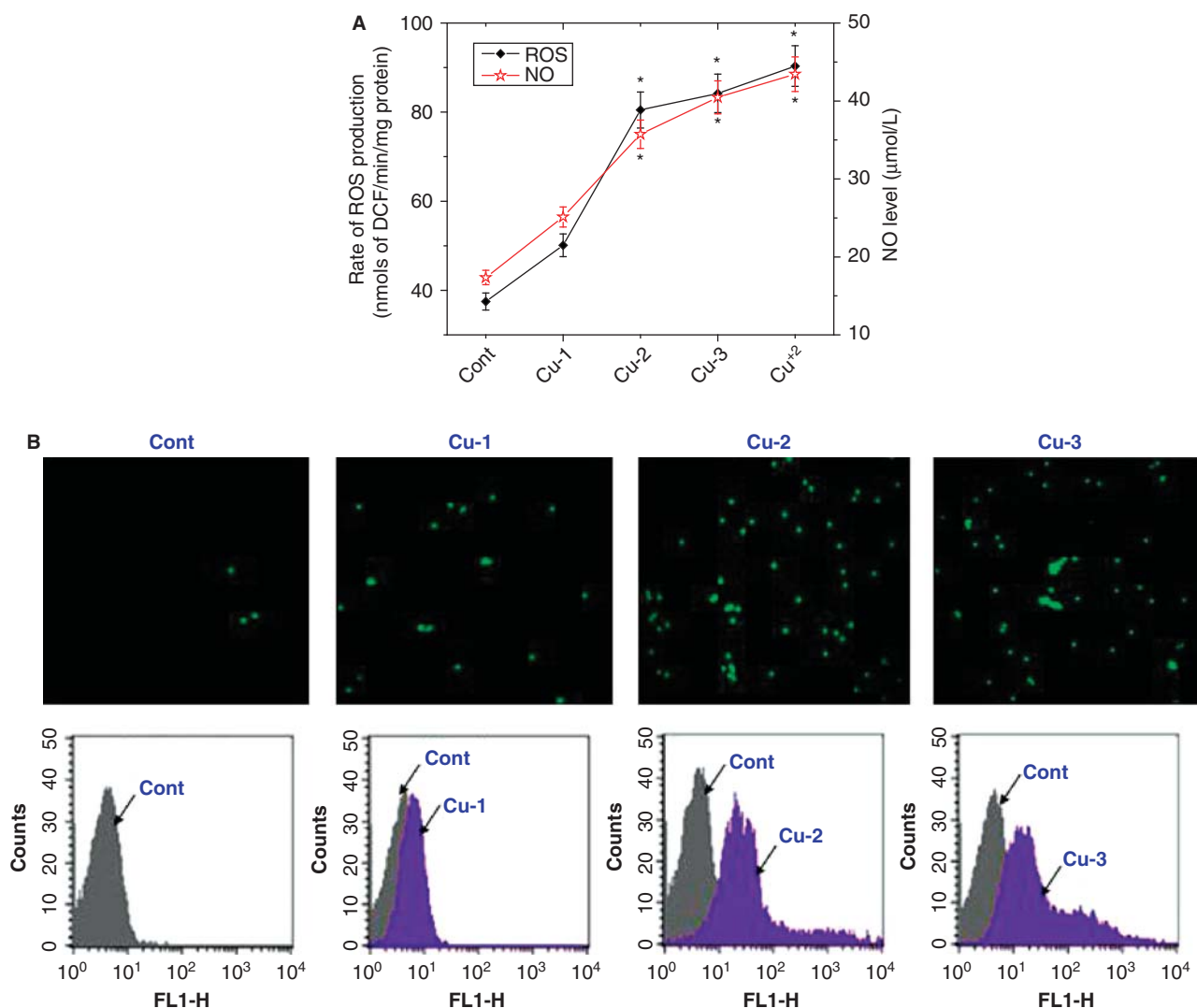


Figure 3. Effect of nano-copper particles and copper ion induced increased production of reactive intermediates. Panel A represents the levels of intracellular reactive intermediates (ROS and NO) in the liver tissue of nano-copper and copper ion exposed animals. Panel B shows the representative images under fluorescence microscope and also the flow cytometric analysis of the nano-copper-intoxicated animals only. Cont: control mice, Cu-1, Cu-2 and Cu-3: animals administered with nano-copper particles at a dose of 200, 413 and 600 mg/kg body weight and Cu²⁺: animals administered with copper chloride at a dose of 110 mg/kg body weight. Data are mean \pm SD, for six animals per group and were analyzed by one-way ANOVA, with Student-Newman-Keuls post-hoc tests. Significant differences (*) were attributed at $p < 0.05$.

Effect on the activity of NF- κ B and I κ B α

NF- κ B, a ubiquitous transcription factor, can be activated by a variety of stimulating signals relevant to pathophysiology. Transcriptional activity of NF- κ B could be regulated by the phosphorylation of I κ B as well as NF- κ B p65 subunits. In our study, we used Western immunoblotting to determine whether activation of NF- κ B and I κ B α are involved in the nano-copper-induced hepatotoxicity. We observed that exposure to nano-copper particles dose-dependently elevated the expression of phosphorylated I κ B α and phosphorylated NF- κ B p65 (Figure 6).

Effect on the activity of mitogen-activated protein kinases (MAPKs)

MAPKs are the upstream critical signaling proteins. There are three distinct subfamilies of MAPKs: Extracellular signal-regulated protein kinase (ERK), p38-MAPK (p38), and c-Jun N-terminal kinase (JNK). To assess the effect of nano-copper exposure on the activation of MAPK subfamilies, the liver tissue homogenates were analyzed for both total and phosphorylated forms of p38, ERK (1/2) and JNK by immunoblotting studies. Figure 7 shows that nano-copper exposure phosphorylated p38

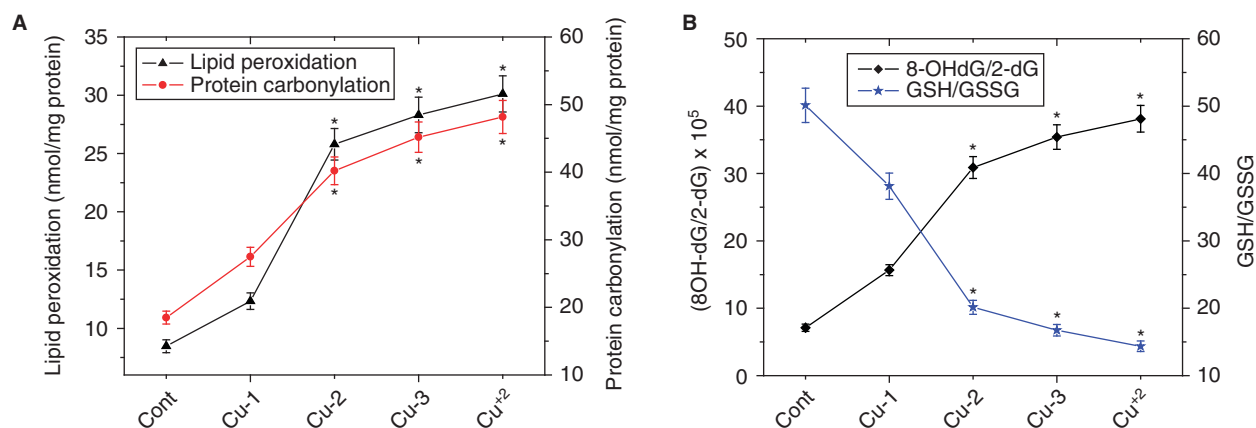


Figure 4. Effect of nano-copper particles and copper ion induced elevated levels of lipid peroxidation as well as protein carbonylation (Panel A) and decreased ratio of GSH/GSSG as well as increased ratio of 8-OHdG/2-dG (Panel B). Cont: control mice, Cu-1, Cu-2 and Cu-3: animals administered with nano-copper particles at a dose of 200, 413 and 600 mg/kg body weight and Cu²⁺: animals administered with copper chloride at a dose of 110 mg/kg body weight. Data are mean \pm SD, for six animals per group and were analyzed by one-way ANOVA, with Student-Newman-Keuls post-hoc tests. Significant differences (*) were attributed at $p < 0.05$.

and ERK, leaving JNK unchanged suggesting the involvement of p38 and ERK in this pathophysiology.

Time-dependent effect on the activities of NF- κ B and MAPKs (p38 and ERK1/2) in response to nano-copper exposure

Figure 8 represents the time-dependent activities of transcription factors, NF- κ B and redox signalling proteins, p38 as well as ERK1/2 in hepatocytes exposed with nano-copper. We found that nano-copper overload increased the translocation of NF- κ B to the nucleus in a time-dependent manner and optimum translocation was observed at about 4 h incubation. However, on the same exposure, phosphorylation of p38 and ERK1/2 started within minute and reached at optimum at about 30 min.

Effect on the Bcl-2 family of proteins

Bcl-2 family proteins are upstream regulator of mitochondrial membrane potential. Figure 9 represents the expressions of Bcl-2 family of proteins. From immunoblotting studies, it has been observed that nano-copper treatment upregulated pro-apoptotic (Bad) and down regulated anti-apoptotic (Bcl-xL) members of Bcl-2 family proteins in liver tissue.

Effect on mitochondria-dependent cell death pathway

Oxidative stress-induced apoptosis is directly related to mitochondrial dysfunction. Disruption of mitochondrial membrane potential and subsequent release of cytochrome C are the novel biomarkers of oxidative stress-induced cell death via mitochondria-dependent pathway. Release of cytochrome C causes activation of

caspsases via the formation of apoptosome. Therefore, we assessed the mitochondrial membrane potential, leakage of cytochrome C into cytosol as well as its level in the mitochondrial fraction and the status of caspsases (initiator caspase 9 and effector caspase 3) and Apaf-1. Flow cytometric analyses showed that nano-copper reduced the mitochondrial membrane potential (Figure 10A) and immunoblot analyses showed the same exposure decreased the level of cytochrome C in the mitochondrial fraction (Figure 10B), elevated the concentration of cytosolic cytochrome C (Figure 10C) and down regulated Apaf-1 (Figure 10D) in association with up-regulating caspase 3 (Figure 10E), cleaved caspase 3 (Figure 10E) and caspase 9 (Figure 10F), indicating the involvement of the mitochondria-dependent signaling cascades in this pathophysiology. Immunofluorescence study (Figure 10G) with isolated hepatocytes also showed that nano-copper exposure elevated the expression of cleaved caspase 3.

Effect of STZ and AA on cell death pathway

To show the apoptotic changes, next we focused on the morphological changes of hepatocytes using DAPI staining. As shown in Figure 11A, hepatocytes from control animals exhibit normal morphology, whereas cells from nano-copper-exposed animals were observed to have condensed chromatin and fragmented nuclei suggesting the nano-copper induced apoptotic cell death.

Finally to understand the percentage of apoptotic cell death, double labeling techniques has been utilized using Annexin V/PI to distinguish between apoptotic and necrotic cells. Flow cytometric data (Figure 11B) revealed that, in comparison with control untreated hepatocytes, nano-copper

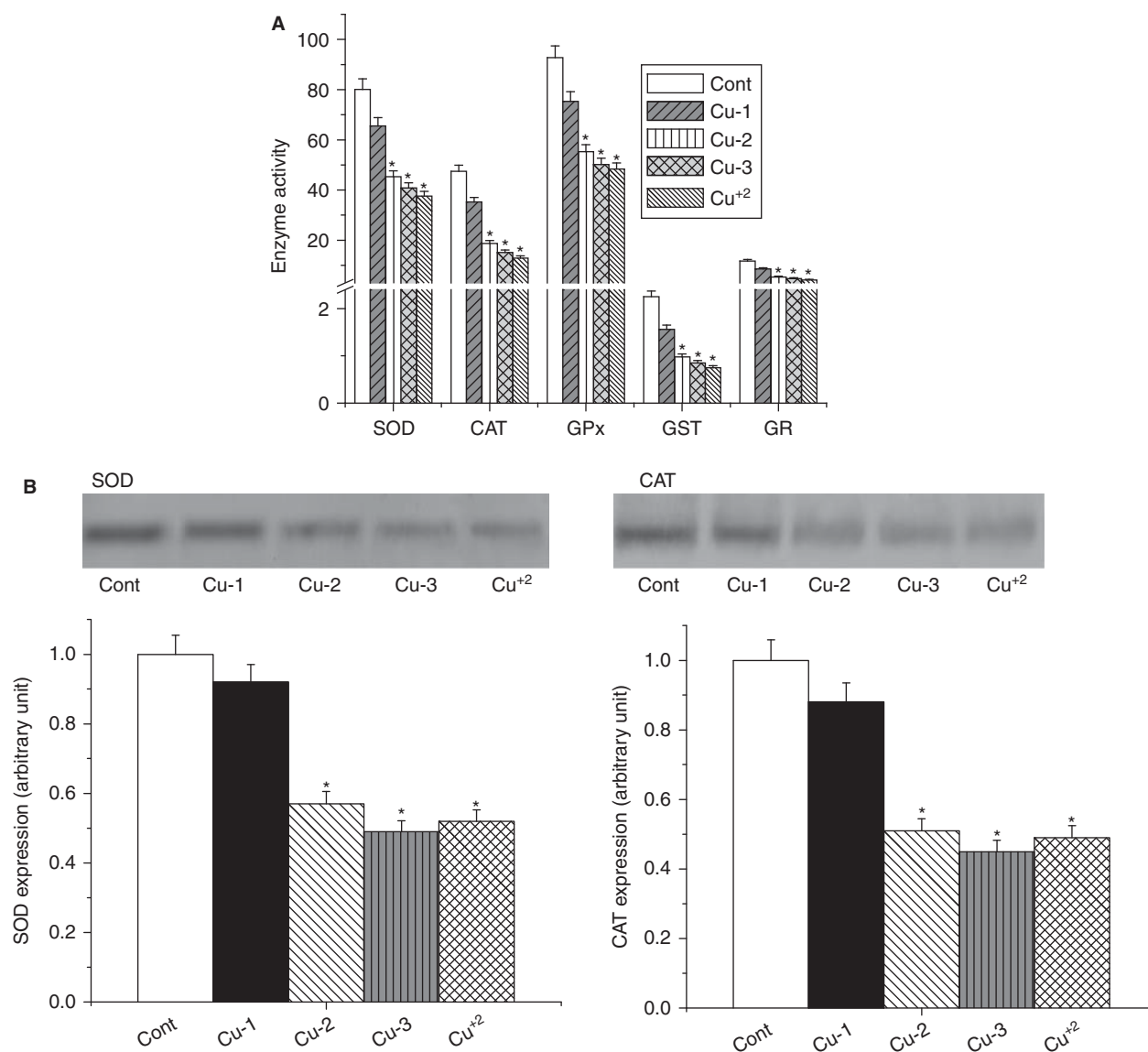


Figure 5. Panel A: Effect of nano-copper particles and copper ion induced decreased activities of antioxidant enzymes. Panel B: Western blot analysis of SOD and CAT in the liver tissue of nano-copper- and copper ion-exposed animals. Cont: control mice, Cu-1, Cu-2 and Cu-3: animals administered with nano-copper particles at a dose of 200, 413 and 600 mg/kg body weight and Cu⁺²: animals administered with copper chloride at a dose of 110 mg/kg body weight. Data are mean \pm SD, for six animals per group and were analyzed by one-way ANOVA, with Student-Newman-Keuls post-hoc tests. Significant differences (*) were attributed at $p < 0.05$. The relative intensities of bands were determined using ImageJ (NIH, USA) software and the control band was given an arbitrary value of 1.

particles-exposure increased the number of Annexin V staining hepatocytes but very little PI binding cells, indicating majority of cells death via the apoptotic pathway.

Histological assessment

Histological assessments of different liver segments of the experimental animals are presented in Figure 12A. Instead of pink-blue image, the color of the Figure 12A is mostly brown and it was due to the tissue condition, staining time and most obviously

photographic exposure time. Hepatic lobular architecture was clear and intact without any abnormalities in the liver section of control group. The most easily recognizable feature of the apoptotic cells is the condensed nuclear chromatin that either appears as a darkly stained single nucleus or a fragmented nucleus (spot of brown/black staining). Intracellular copper overload caused obvious swelling of liver cells, chromatin condensation and formation of apoptotic bodies. The apoptotic cells may also be seen within vacuoles (with an apparently empty space surrounding the apoptotic bodies within the vacuole) inside

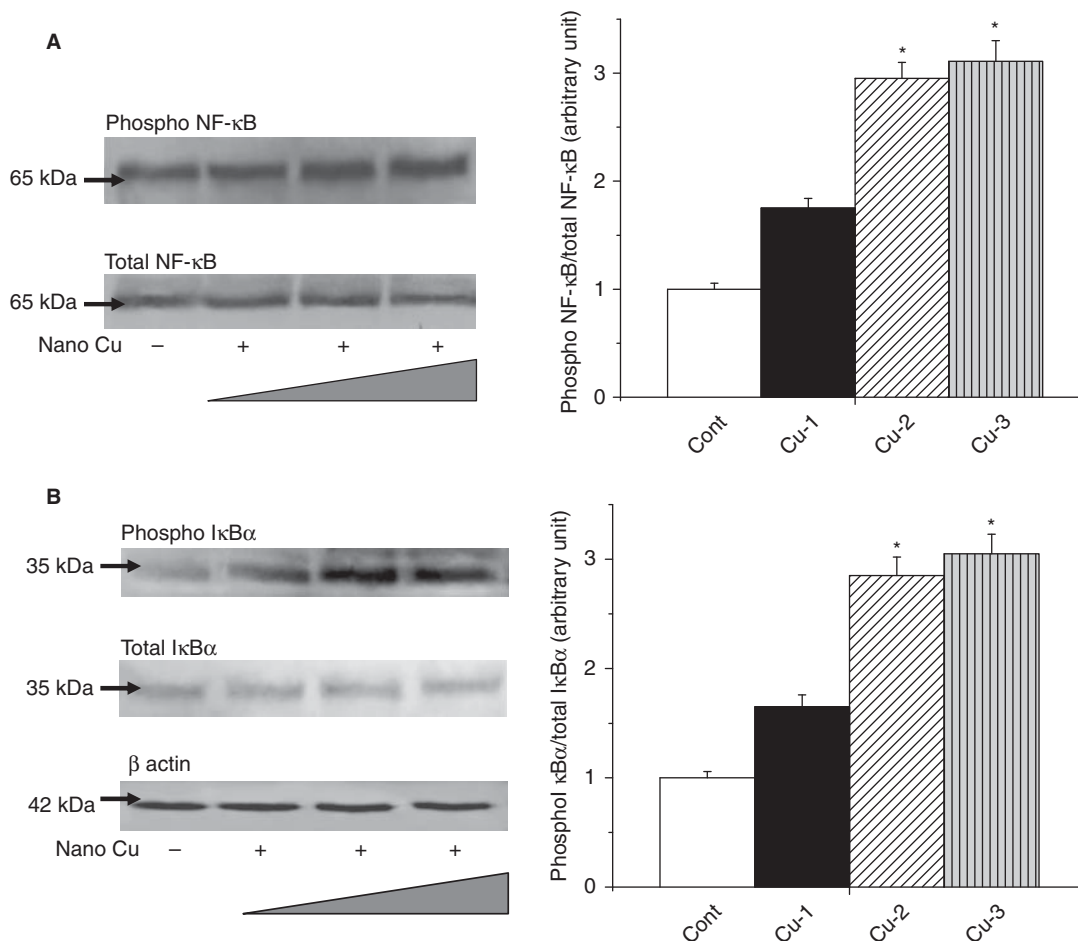


Figure 6. Western blot analysis of NF- κ B (Panel A) and I κ B α (Panel B) in the liver tissue of nano-copper-intoxicated animals. The relative intensities of bands were determined using ImageJ (NIH, USA) software and the control band was given an arbitrary value of 1. Cont: control mice, Cu-1, Cu-2 and Cu-3: animals administered with nano-copper particles at a dose of 200, 413 and 600 mg/kg body weight. Data are mean \pm SD, for six animals per group and were analyzed by one-way ANOVA, with Student-Newman-Keuls post-hoc tests. Significant differences (*) were attributed at $p < 0.05$.

neighboring cells (macrophages in the germinal centers). Immunohistochemical study (Figure 12B) with anti cleaved caspases 3 antibody revealed the significant increased expression of cleaved caspases 3 (dark blue/black staining on the pinkish blue background) in the liver tissue of the nano-copper-exposed animals and this observation clearly suggests that the nano-copper-induced apoptotic cell death occurs via caspases 3 dependent pathways. Increased appearance of dark blue/black balls also indicated the nucleus fragmentation in the nano-copper-treated sections of Figure 12B. Over expression of cleaved caspase 3 was less pronounced in the liver section of the control.

Discussion

Liver is the primary target organ for nearly all drugs and toxic chemicals because it plays an

important role for the metabolism of those harmful xenobiotics. Excessive exposure to these chemicals may cause acute liver injury characterized by abnormality of hepatic function, and degeneration, necrosis or apoptosis of hepatocytes, etc. Beside the widely accepted benefits of nanotechnology, potential adverse effect of nanomaterials on human health is a serious clinical problem. Extensive research works have been carried out to investigate the optimum dose, routes of exposure as well as the mechanism of nanoparticles-induced organ pathophysiology (Mohanraj and Chen 2006). The present study demonstrates the nano-copper particles induced hepatotoxicity and hepatocyte cell death via the activation of oxidative stress-responsive cell signaling pathways.

Reduction in the hepatic index and increased activities of the serum marker enzymes ALT, ALP are the two important physiological indices for hepatic

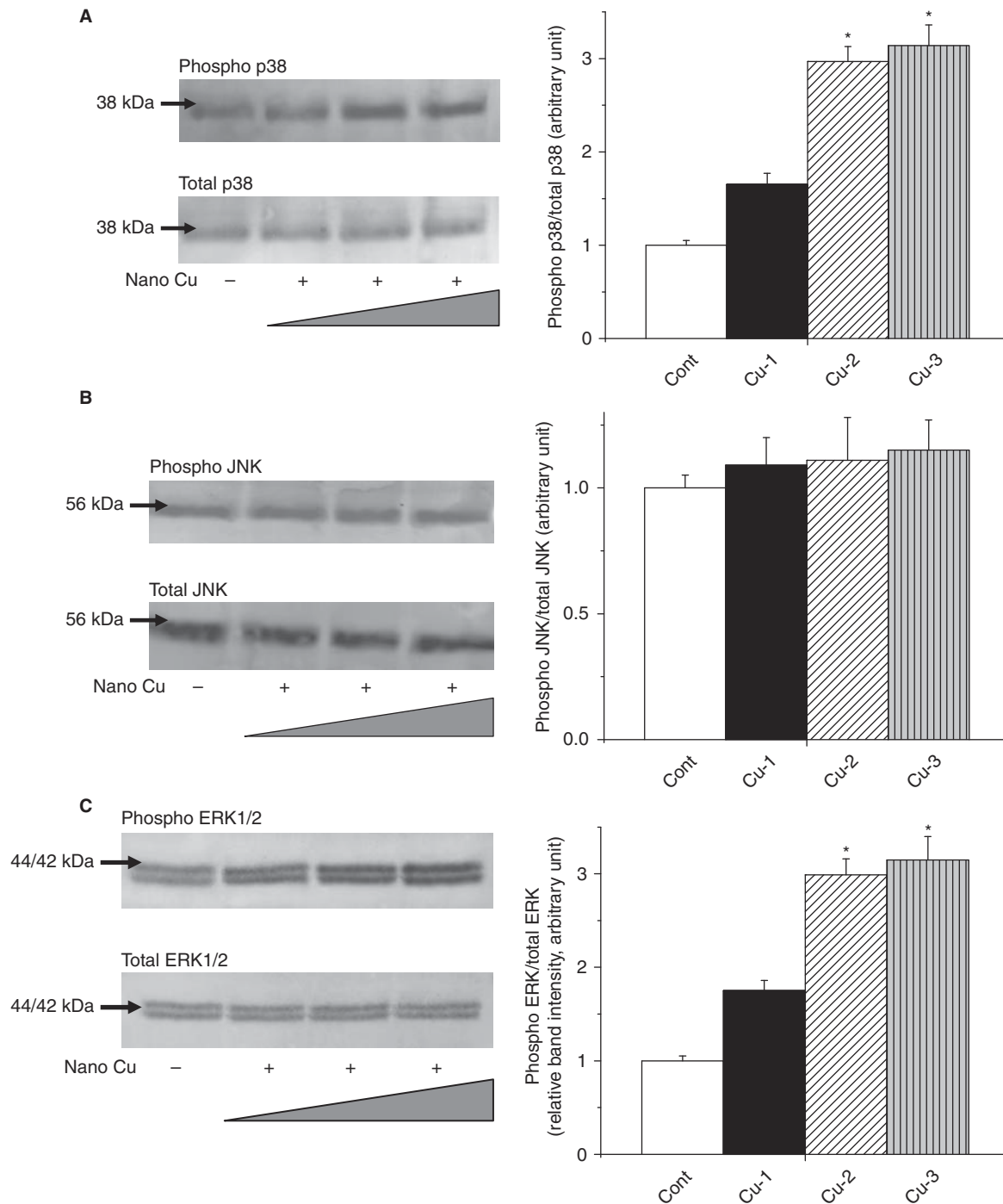


Figure 7. Western blot analysis of MAPKs (p38: Panel A; JNK: Panel B; ERK1/2: Panel C) in the liver tissue of nano-copper-intoxicated animals. The relative intensities of bands were determined using ImageJ (NIH, USA) software and the control band was given an arbitrary value of 1. Cont: control mice, Cu-1, Cu-2 and Cu-3: animals administered with nano-copper particles at a dose of 200, 413 and 600 mg/kg body weight. Data are mean \pm SD, for six animals per group and were analyzed by one-way ANOVA, with Student-Newman-Keuls post-hoc tests. Significant differences (*) were attributed at $p < 0.05$.

pathophysiology. Administration of nano-copper particles (400 mg/kg body weight) caused a dramatic atrophy of the liver and thus reduced the hepatic index of experimental animals. Administration of toxins and

drugs cause hepatocytes injury and that alters the membrane permeability, leading to the leakage of membrane-bound enzymes from these cells. Exposure to nano-copper particles also caused

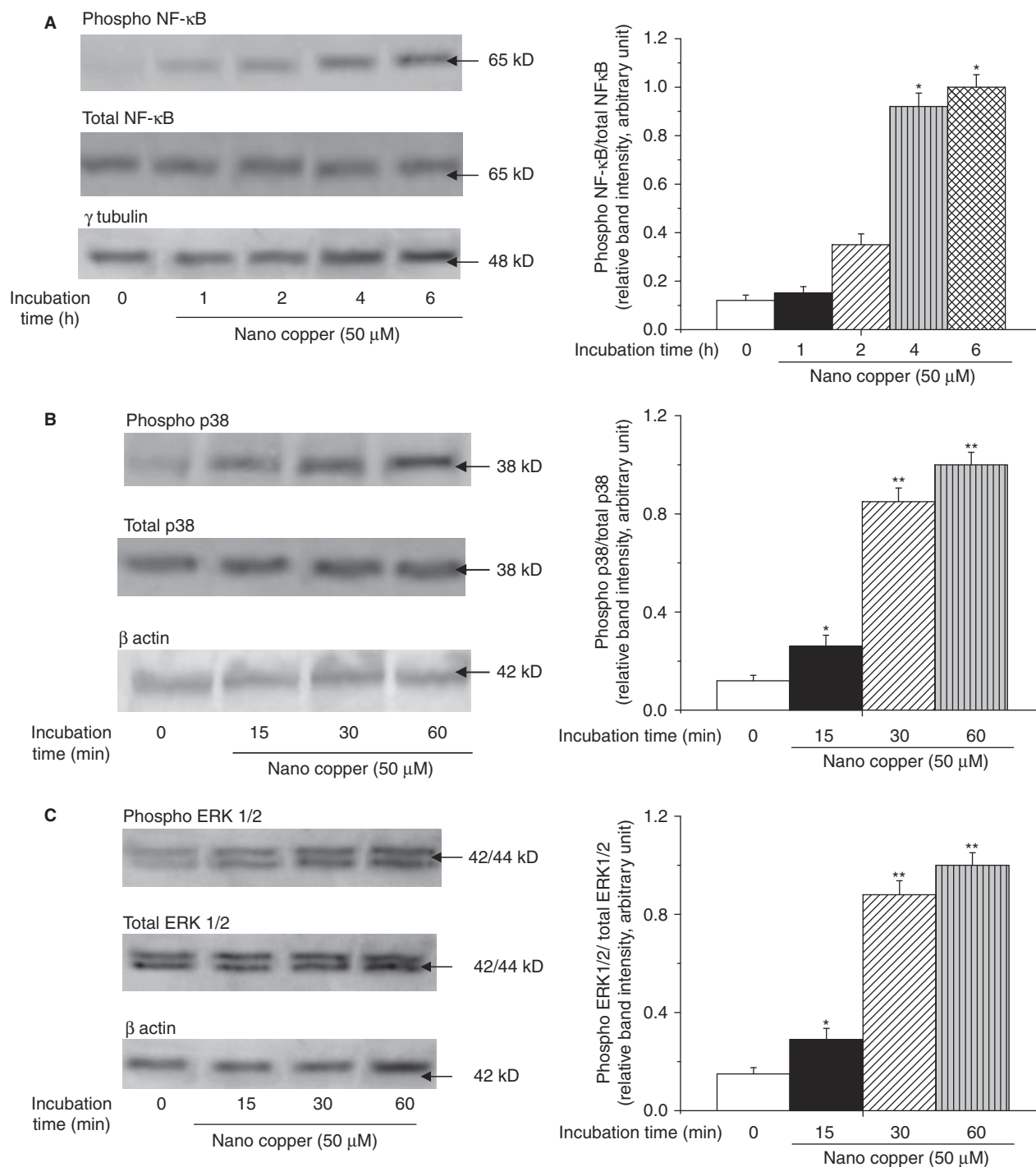


Figure 8. Time-dependent Western blot analysis of NF-κB (Panel A) and MAPKs (p38: Panel B and ERK1/2: Panel C) in the isolated hepatocytes exposed with nano-copper (50 μM) for different time periods. The relative intensities of bands were determined using ImageJ (NIH, USA) software. Data are mean ± SD, $n = 6$ and were analyzed by one-way ANOVA, with Student-Newman-Keuls post-hoc tests. Significant differences (*) were attributed at $p < 0.05$.

hepato-cellular damage, as evident from the increased activities of ALT and ALP in the sera of experimental animals.

It is reported that after exposure, nano-copper particles enter into the gastric lumen where they

rapidly react with the hydrogen ions of the gastric juice and convert into its ionic states (Chen et al. 2006) (Figure 12). The large surface area causes the ultrahigh reactivity of the nano-sized copper particles. The depletion of hydrogen ions results in metabolic

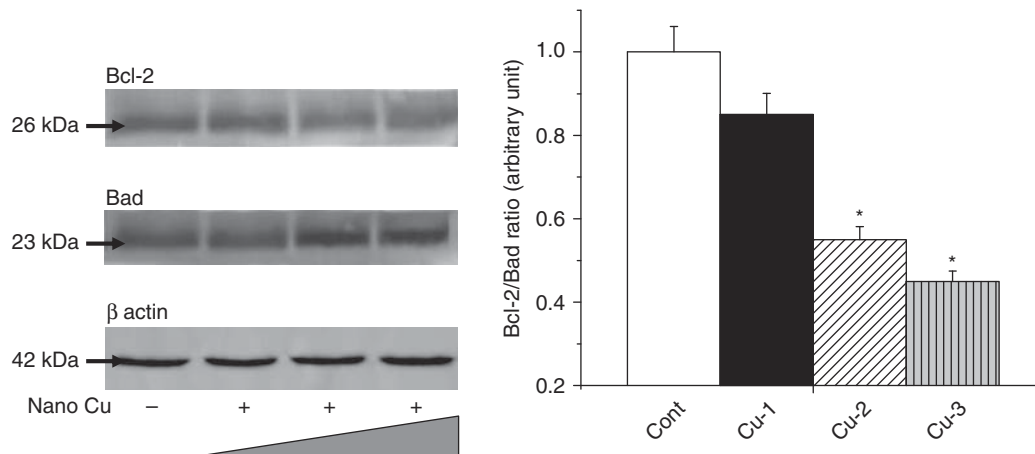


Figure 9. Western blot analysis of Bad and Bcl-2 in the liver tissue of nano-copper-intoxicated animals. The relative intensities of bands were determined using ImageJ (NIH, USA) software and the control band was given an arbitrary value of 1. Cont: control mice, Cu-1, Cu-2 and Cu-3: animals administered with nano-copper particles at a dose of 200, 413 and 600 mg/kg body weight. Data are mean \pm SD, for six animals per group and were analyzed by one-way ANOVA, with Student-Newman-Keuls post-hoc tests. Significant differences (*) were attributed at $p < 0.05$.

alkalosis because the bicarbonate ions generated during production of gastric acid will return to the circulation, resulting in the formation of large quantities of sodium bicarbonate which increase the arterial blood pH. Elevated blood pH level motivates a series of pathological abnormalities like respiratory complications, renal compensations, etc. The strong ionization potential of nano-copper particles helps in the development of copper ion overload which damages the hepatic cells, causes the lipodystrophy as well as steatosis and increases the ALP and TBA levels in blood. Thus both copper ion overload and metabolic alkalosis contribute to the toxicity of nano-copper particles.

Earlier studies (Krumschnabel et al. 2005) reported that copper ions overload cause the disruption of Ca^{+2} homeostasis and increases the formation of ROS. Stimulation of ROS production causes oxidative stress which plays an important role in the pathogenesis and progression of nano-copper particles-induced liver diseases (Meng et al. 2007). In our study, we observed that exposure to copper nanoparticles dose-dependently increased the intracellular ROS and NO production. Both oxidative and nitrosative stress altered the enzymatic and non-enzymatic antioxidant defense. In this context, we assayed the activities of the antioxidant enzymes SOD, CAT, GST, GR, GPx and G6PD and the levels of the non-enzymatic antioxidant molecules GSH and its metabolite GSSG. Production of increased free radicals caused the oxidation of DNA molecules. We observed that intracellular copper ions overload decreased the activities of the antioxidant enzymes, the GSH/GSSG as well as 8-OHdG/2-dG ratios along with increased lipid peroxidation and protein carbonylation.

Oxidative stress induces the transcription of a variety of genes involved in the detoxification of ROS, or in the repair of ROS-induced damage. Increased production of ROS activates the redox sensitive transcription factors (TFs) [nuclear factor- κ B (NF- κ B) and activator protein-1 (AP-1)] induced signal transduction pathways which in turn leads to transcription of genes involved in the cell growth regulatory pathways. NF- κ B has been implicated in the gene regulation, related to cell proliferation, apoptosis, adhesion, immune and inflammatory responses (Baldwin 1996). The NF- κ B transcriptional factors are composed of homodimers or heterodimers of Rel protein, of which, p65/p50 is the predominant complex. Phosphorylation at the multiple serine sites of p65 subunit increases the transcriptional activity of NF- κ B in the nucleus where it binds to the DNA and induces gene expression (Akira and Kishimoto 1997). Transcriptional activity of NF- κ B could also be regulated by the phosphorylation of inhibitor- κ B (I κ B) (Sakurai et al. 2003). Removal of I κ B induces translocation of NF- κ B into the nucleus. Transcriptional activity of NF- κ B is thus regulated by the phosphorylation of I κ B as well as its p65 subunit. In the present study, we observed that intracellular copper burden caused NF- κ B activation (p65 sub unit) which is linked with the simultaneous increased phosphorylation of I κ B α .

Genes, regulated by TFs, are in turn controlled by the mitogen-activated protein kinase (MAPK) signaling cascades. MAPKs are a family of serine/threonine kinases that are activated by dual phosphorylation on threonine and tyrosine residues. The three MAPK pathways; ERK, JNK and p38; transduce intra- and extra-cellular stimuli, which lead to diverse

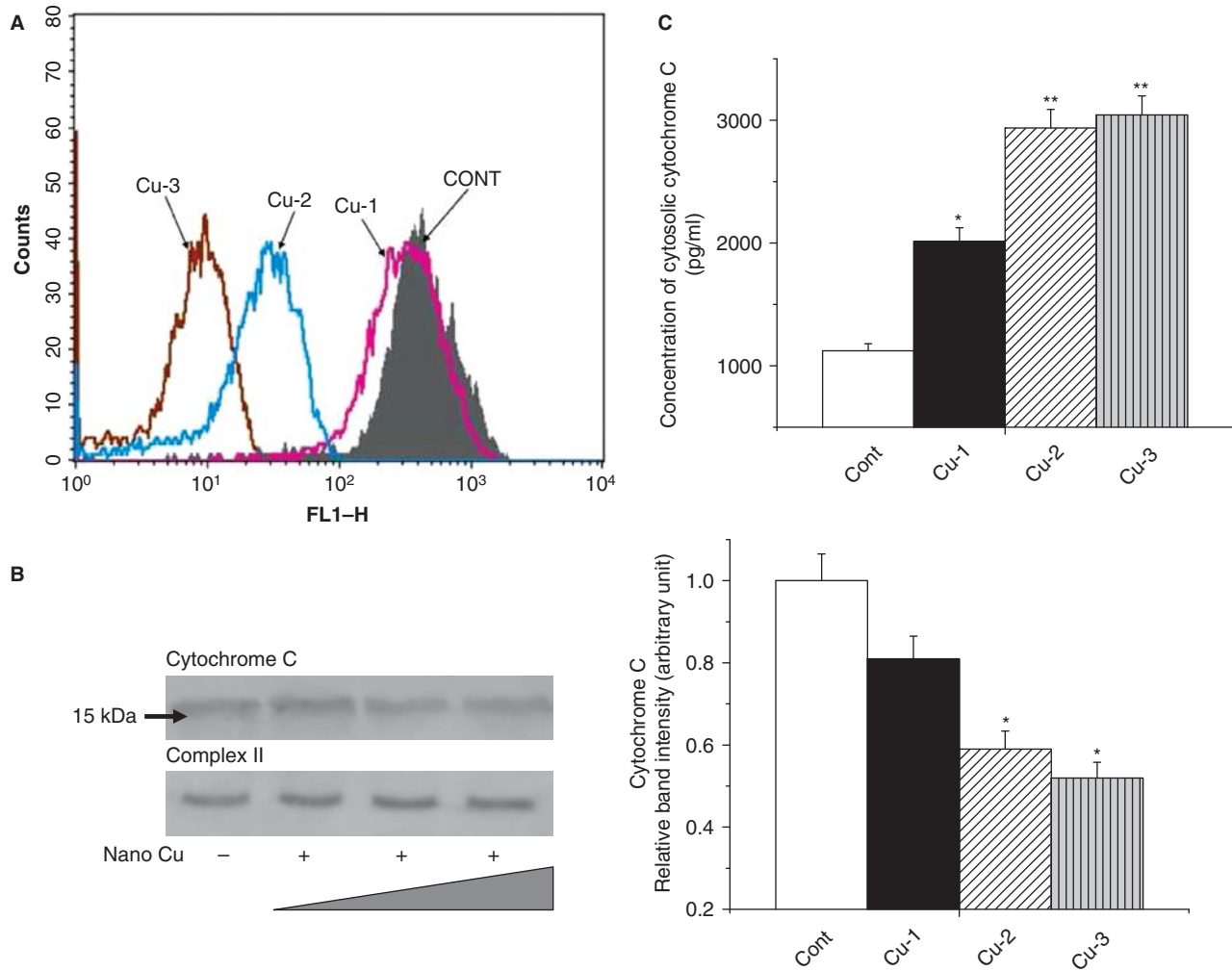


Figure 10. (A) Study on the mitochondrial membrane potential by flow cytometry analysis. Cont: mitochondria isolated from the liver tissue of control animals; Cu-1, Cu-2 and Cu-3: mitochondria isolated from the liver tissue of the animals administered with nano-copper particles at a dose of 200, 413 and 600 mg/kg body weight. (B) Western blot analysis of cytochrome C in the mitochondrial fraction of the liver tissue of nano-copper-intoxicated animals. The relative intensities of bands were determined using ImageJ (NIH, USA) software and the control band was given an arbitrary value of 1. Cont: control mice, Cu-1, Cu-2 and Cu-3: animals administered with nano-copper particles at a dose of 200, 413 and 600 mg/kg body weight. Data are mean \pm SD, of six separate experiments in each group and were analyzed by one-way ANOVA, with Student-Newman-Keuls post-hoc tests. Significant differences (*) were attributed at $p < 0.05$. The purity of mitochondrial fraction was checked by immunoblotting analysis with anti complex II antibody. (C) Study on the concentration of cytosolic cytochrome C. Cont: control mice, Cu-1, Cu-2 and Cu-3: animals administered with nano-copper particles at a dose of 200, 413 and 600 mg/kg body weight. Data are mean \pm SD, of six separate experiments in each group and were analyzed by one-way ANOVA, with Student-Newman-Keuls post-hoc tests. Significant differences (*) were attributed at $p < 0.05$. (D) Western blot analysis of Apaf-1 in the liver tissue of nano-copper-intoxicated animals. The relative intensities of bands were determined using ImageJ (NIH, USA) software and the control band was given an arbitrary value of 1. Cont: control mice, Cu-1, Cu-2 and Cu-3: animals administered with nano-copper particles at a dose of 200, 413 and 600 mg/kg body weight. Data are mean \pm SD, of six separate experiments in each group and were analyzed by one-way ANOVA, with Student-Newman-Keuls post-hoc tests. Significant differences (*) were attributed at $p < 0.05$. (E and F) Western blot analysis of caspase 3 (E), cleaved caspase 3 and caspase 9 (F) in the liver tissue of nano-copper-intoxicated animals. The relative intensities of bands were determined using ImageJ (NIH, USA) software and the control band was given an arbitrary value of 1. Cont: control mice, Cu-1, Cu-2 and Cu-3: animals administered with nano-copper particles at a dose of 200, 413 and 600 mg/kg body weight. Data are mean \pm SD, of six separate experiments in each group and were analyzed by one-way ANOVA, with Student-Newman-Keuls post-hoc tests. Significant differences (*) were attributed at $p < 0.05$. (G) Representative confocal microscopy images ($\times 200$). The activation of the apoptotic program was assessed by measuring fluorescence changes in cleaved caspase-3 (green fluorescence) activity. Cont: control mice, Cu-1, Cu-2 and Cu-3: animals administered with nano-copper particles at a dose of 200, 413 and 600 mg/kg body weight.

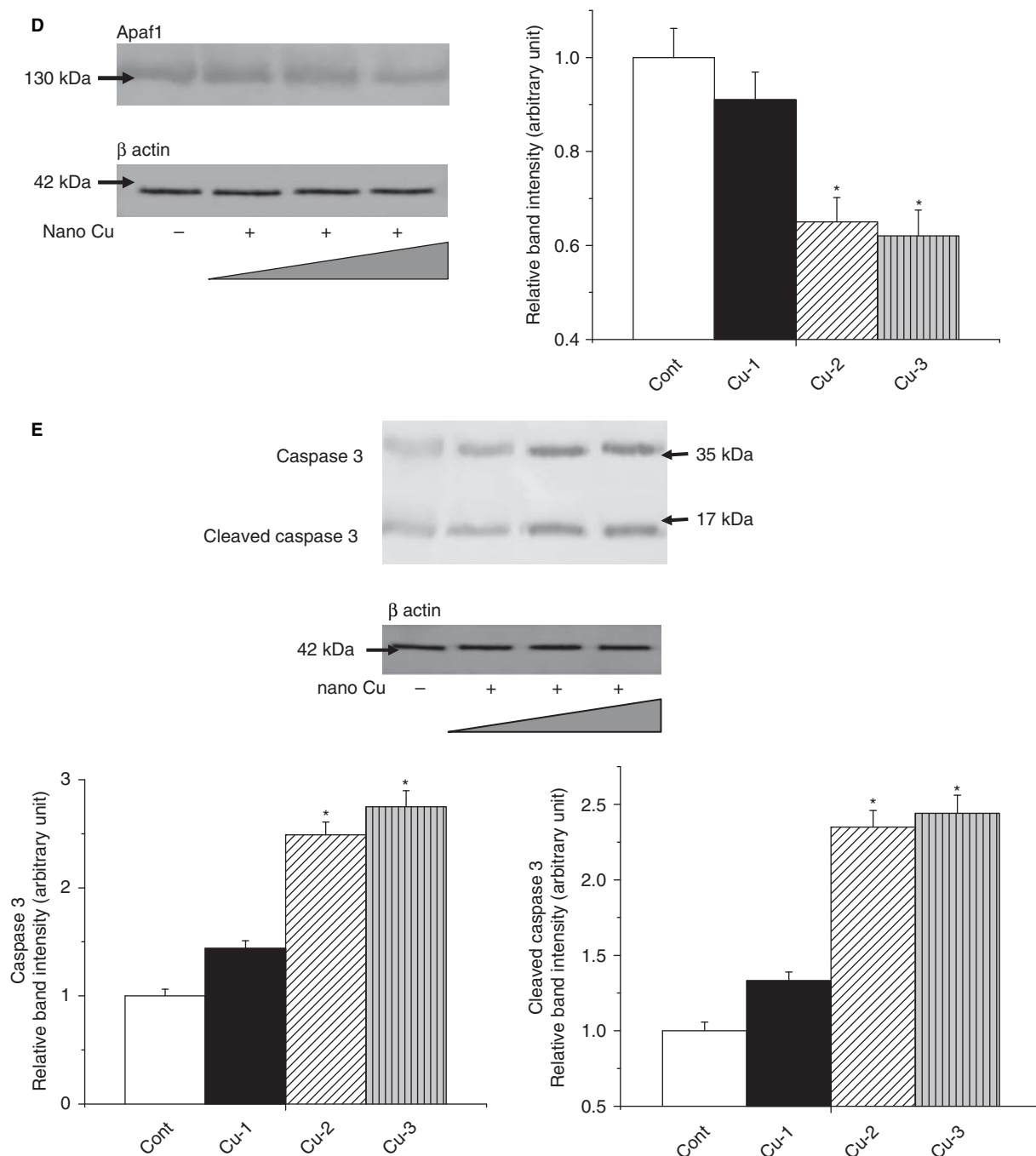


Figure 10. (Continued).

cellular responses. The ERK pathway typically responds to the growth factor signals, which leads to cell differentiation or proliferation. In contrast, the JNK and p38 pathways respond to cytokines and cellular stress; resulting in the transcriptional activation of genes involved in stress responses, growth arrest or apoptosis. In the present study we observed that intracellular copper overload caused dose-dependent activation of phosphorylated ERK as

well as phosphorylated p38 leaving the activation of JNK unchanged. Studies on isolated hepatocytes with nano-copper exposure (50 μ M) revealed that phosphorylation of p38 and ERK1/2 started within minutes.

Apoptosis is known to be a delicately controlled programmed cell death pathway. Cumulative evidences suggest that the alteration in mitochondrial membrane potential is able to switch the committed

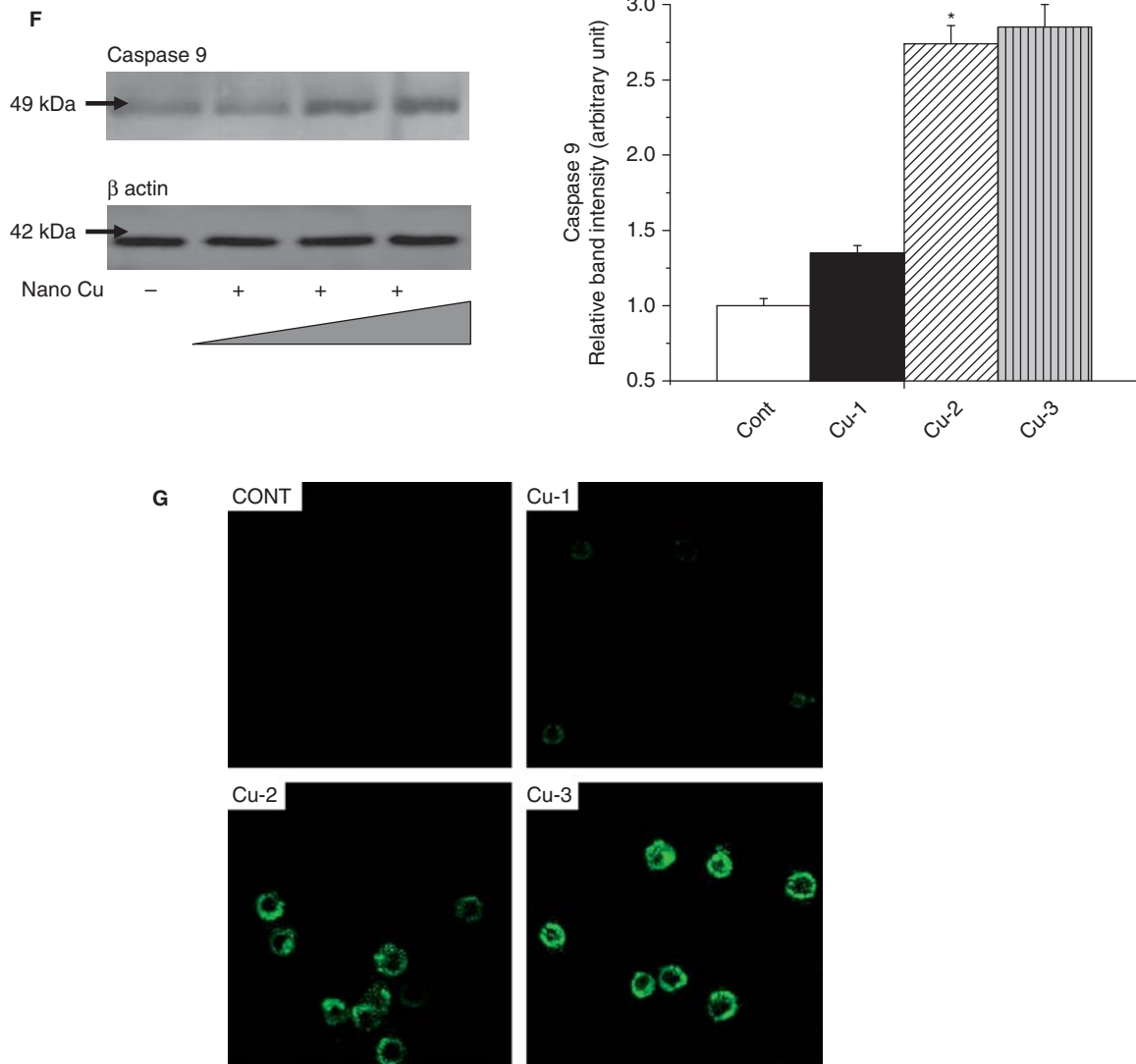


Figure 10. (Continued).

cells to apoptotic death via oxidative stress responsive signaling cascades (Keeble and Gilmore 2007). Verzola et al. (2002) reported the influence of Bcl-2 family proteins on the mitochondria to regulate the mitochondria-dependent cell death. There are two classes of reciprocal regulatory proteins in the Bcl-2 family: The anti-apoptotic members (e.g., Bcl-2, Bcl-xL) protect the cells from apoptosis, whereas the pro-apoptotic members (e.g., Bax, Bad) promote the programmed cell death. Action of Bcl-2 family proteins on mitochondria causes the release of cytochrome C from mitochondria to the cytosol. In the cytosol, cytochrome C interacts with Apaf1 and procaspase-9 to form the apoptosome that triggers the activation of caspase-3. In our study we investigated the role of Bcl-2 family proteins and the mitochondria-dependent signal transduction pathways in nano-copper particles-induced hepatocyte

cell death. We observed that exposure to nano-copper particles up-regulated the pro-apoptotic (Bad) and down-regulated anti-apoptotic (Bcl-2) members of Bcl-2 proteins. Alteration in the Bcl-2/Bad ratio caused reduction in mitochondrial membrane potential, release of cytochrome C followed by the decreased level of Apaf-1 in the cytosol. Nano-copper particles induced loss in mitochondrial membrane potential and formation of apoptosome subsequently activated the cell death executor caspases (caspase 3 and caspase 9). Immunofluorescence study, (using anti-caspase 3 and anti-Apaf 1) also supports our immunoblot analyses.

Results from immunoblot and immunocytochemistry studies suggest that intracellular copper burden induced hepatic cell death mostly via the apoptotic pathway (Figure S1, available online). In agreement with the cell signaling data, studies under confocal

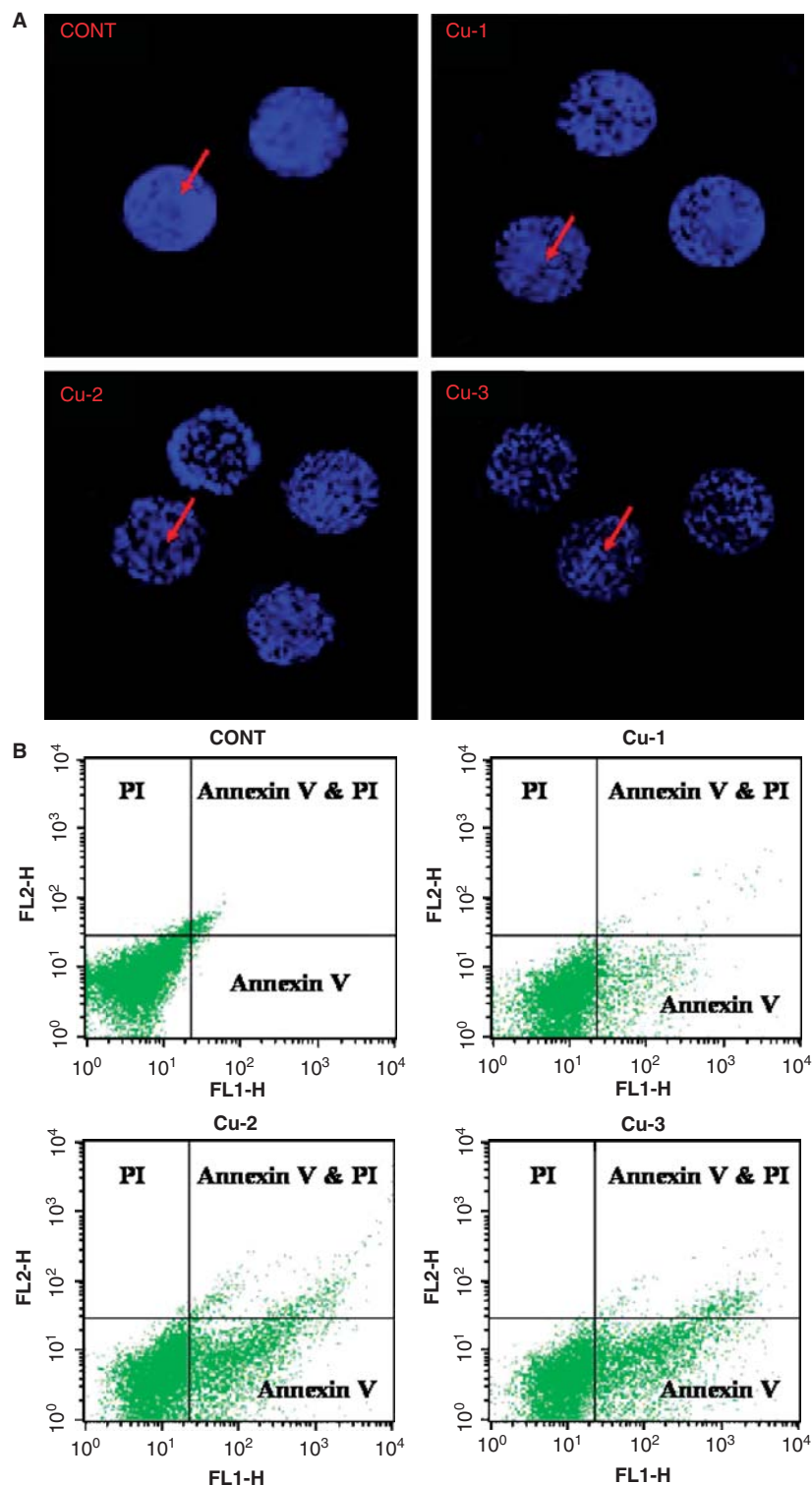


Figure 11. (A) Confocal imaging of DAPI staining ($\times 1000$). Apoptotic cells were imaged by using DAPI (blue) fluorescent probe. Cont: cells isolated from the liver tissue of control animals; Cu-1, Cu-2 and Cu-3: cells isolated from the liver tissue of animals administered with nano-copper particles at a dose of 200, 413 and 600 mg/kg body weight. (B) Effect of nano-copper particles on percentage distribution of apoptotic and necrotic cells. Cell distribution analyzed using Annexin V binding and PI uptake. The FITC and PI fluorescence measured using flow cytometer with FL-1 and FL-2 filters, respectively. Results expressed as dot plot representing as one of the six independent experiments. Cont: cells isolated from the liver tissue of control animals; Cu-1, Cu-2 and Cu-3: cells isolated from the liver tissue of animals administered with nano-copper particles at a dose of 200, 413 and 600 mg/kg body weight.

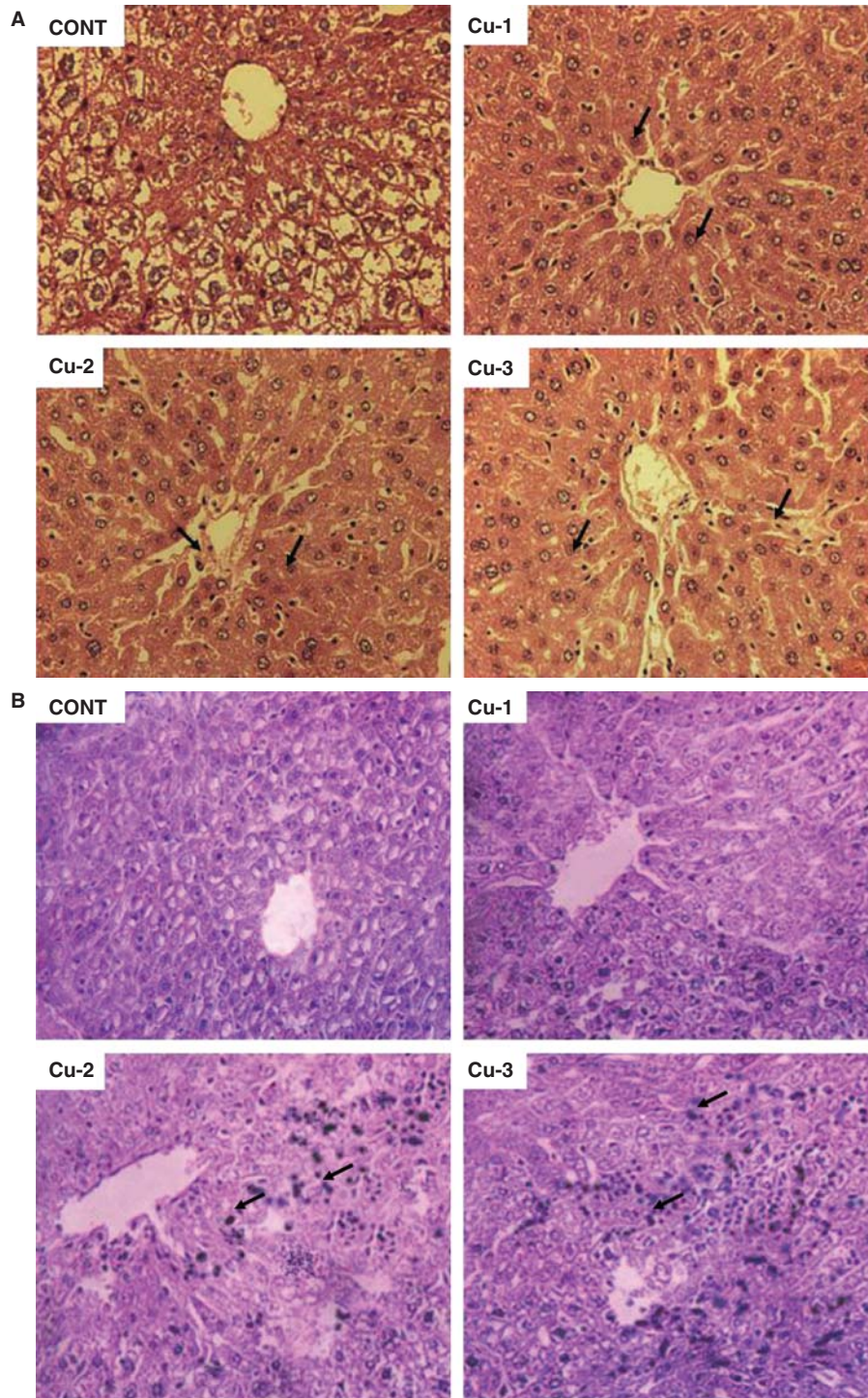


Figure 12. (A) Histopathological changes in liver tissue (stained with haematoxylin and eosin dye). Cont: liver section of control ($\times 400$); Cu-1, Cu-2 and Cu-3: liver section of animals administered with nano-copper particles at a dose of 200, 413 and 600 mg/kg body weight, arrows indicate the apoptotic changes (spot of brown/black staining). (B) Immunohistochemistry with the antibodies for cleaved caspases 3. Cont: liver section of control ($\times 200$); Cu-1, Cu-2 and Cu-3: liver section of animals administered with nano-copper particles at a dose of 200, 413 and 600 mg/kg body weight, showing increased expression of cleaved caspases 3 marked with dark blue or black spot ($\times 200$) (arrows indicate).

microscope (using DAPI staining) revealed that exposure to nano-copper particles elevated the chromatin condensation as well as increased the numbers of fragmented nuclei. Finally FACS analysis with Annexin V/PI double staining showed dose-dependent increased population of apoptotic cell death. In agreement with the above findings, histological assessments revealed that intracellular copper overload increased the formation of apoptotic bodies as well as nuclear chromatin condensation around the edge of the nucleus.

The results of our study suggest that nano-copper-induced oxidative hepatic dysfunction is similar to that of the copper ion exposure. Literature (Chen et al. 2006) suggests that after intake, nano-copper particles are rapidly converted to the copper ion and thus increase the intracellular copper burden. In conclusion, we would, therefore, like to mention that intercellular copper overload (mediated by nano-copper particles via copper ion formation) caused liver dysfunction as well as hepatic cell death mostly via apoptotic pathways and mediated by oxidative stress-induced cell signaling cascades including the signals from mitochondria. To the best of our knowledge, this is probably the first report in describing the detail mechanism of nano-copper-induced hepatic pathophysiology and may provide information about the safety and care that should be taken before using nano-copper in nanomedicine.

Acknowledgements

The authors are grateful to Mr Prasanta Pal for excellent technical assistance for the study.

Declaration of interest: The authors report no conflict of interest. The authors alone are responsible for the content and writing of the paper.

References

- Akira S, Kishimoto T. 1997. NF-IL6 and NF- κ B in cytokine gene regulation. *Adv Immunol* 65:1–46.
- Bai J, Rodriguez AM, Melendez JA, Cederbaum AI. 1999. Overexpression of catalase in cytosolic or mitochondrial compartment protects HepG2 cells against oxidative injury. *J Biol Chem* 274:26217–26224.
- Baldwin AS. 1996. The NF- κ B and I κ B proteins: New discoveries and insights. *Annu Rev Immunol* 14:649–683.
- Bjorn PZ, Hermann HD, Max L, Heide S, Barabara KG, Hartmut D. 2003. Epidemiological investigation on chronic copper toxicity to children exposed via the public drinking water supply. *Sci Total Environ* 302:127–144.
- Bradford MM. 1976. A rapid and sensitive method for the quantitation of microgram quantities of protein utilizing the principle of protein-dye binding. *Anal Biochem* 72:248–254.
- Chen Z, Meng H, Yuan H, Xing G, Chen C, Zhao F, et al. 2007. Identification of target organs of copper nanoparticles with ICP-MS technique. *J Radioanal Nucl Chem* 272:599–603.
- Chen Z, Meng H, Xing G, Chen C, Zhao Y, Jia G, et al. 2006. Acute toxicological effects of copper nanoparticles in vivo. *Toxicol Lett* 163:109–120.
- Cioffi N, Ditaranto N, Torsi L, Picca RA, Sabbatini L, Valentini A, Novello L, Tantillo G, Bleve-Zacheo T, Zambonin PG. 2005. Analytical characterization of bioactive fluoropolymer ultra-thin coatings modified by copper nanoparticles. *Anal Bioanal Chem* 381:607–616.
- Georgopoulos PG, Roy A, Yonone-Lioy MJ, Opiekun RE, Lioy PJ. 2001. Environmental copper: Its dynamics and human exposure issues. *J Toxicol Environ Health* 4:341–394.
- Ghosh A, Sil PC. 2009. Protection of acetaminophen induced mitochondrial dysfunctions and hepatic necrosis via Akt-NF- κ B pathway: Role of a novel plant protein. *Chem Biol Interact* 177:96–106.
- Guo K, Pan Q, Wang L, Fang S. 2002. Nano-scale copper-coated graphite as anode material for lithium-ion batteries. *J Appl Electrochem* 32:679–685.
- Hevel JM, Marietta MA. 1994. Nitric-oxide synthase assays. *Methods Enzymol* 233:250–258.
- Kasai H, Crain PF, Kuchino Y, Nishimura S, Ootsuyama A, Tanooka H. 1986. Formation of 8-hydroxyguanine moiety in cellular DNA by agents producing oxygen radicals and evidence for its repair. *Carcinogenesis* 7:1849–1851.
- Keeble JA, Gilmore AP. 2007. Apoptosis commitment – translating survival signals into decisions on mitochondria. *Cell Res* 17:976–984.
- Kim JD, McCarter RJM, Yu BP. 1996. Influence of age, exercise and dietary restriction on oxidative stress in rats. *Aging Clin Exp Res* 8:123–129.
- Kipen HM, Laskin DL. 2005. Smaller is not always better: nanotechnology yields nanotoxicology. *Am J Physiol* 289:696–697.
- Krumschnabel G, Manzl C, Berger C, Hofer B. 2005. Oxidative stress, mitochondrial permeability transition, and cell death in Cu-exposed trout hepatocytes. *Toxicol Appl Pharmacol* 209:62–73.
- LeBel CP, Bondy SC. 1990. Sensitive and rapid quantitation of oxygen reactive species formation in rat synaptosomes. *Neurochem Int* 17:435–440.
- Liu G, Li X, Qin B, Xing D, Guo Y, Fan R. 2004. Investigation of the mending effect and mechanism of copper nanoparticles on a tribologically stressed surface. *Tribol Lett* 17:961–966.
- Manna P, Sinha M, Sil PC. 2009. Protective role of arjunolic acid in response to streptozotocin-induced type-I diabetes via the mitochondrial dependent and independent pathways. *Toxicology* 257:53–63.
- Meng H, Chen Z, Xing G, Yuan H, Chen C, Zhao F, et al. 2007. Ultrahigh reactivity provokes nanotoxicity: explanation of oral toxicity of nano-copper particles. *Toxicol Lett* 175:102–110.
- Mohanraj VJ, Chen Y. 2006. Nanoparticles – a review. *Trop J Pharm Res* 5:561–573.
- Nawaz M, Manzl C, Lacher V, Krumschnabel G. 2006. Copper-induced stimulation of extracellular signal-regulated kinase in trout hepatocytes: The role of reactive oxygen species, Ca^{2+} , and cell energetics and the impact of extracellular signal-regulated Kinase signaling on apoptosis and necrosis. *Tox Sci* 92:464–475.
- Oberdörster G, Oberdörster E, Oberdörster J. 2005. Nanotoxicology: An emerging discipline evolving from studies of ultrafine particles. *Environ Health Perspect* 113:823–839.
- Oberdörster G, Stone V, Donaldson K. 2007. Toxicology of nanoparticles: A historical perspective. *Nanotoxicology* 1:2–25.

- Ozcelik D, Ozaras R, Gurel Z, Uzun H, Aydin S. 2003. Copper-mediated oxidative stress in rat liver. *Biol Trace Elem Res* 96:209–215.
- Sakurai H, Suzuki S, Kawasaki N, Nakano H, Okazaki T, Chino A, Doi T, Saiki I. 2003. Tumor necrosis factor- α -induced IKK phosphorylation of NF-kappaB p65 on serine 536 is mediated through the TRAF2, TRAF5, and TAK1 signaling pathway. *J Biol Chem* 278:36916–36923.
- Valen G, Hansson GK, Dumitrescu A, Vaage J. 2000. Unstable angina activates myocardial heat shock protein 72, endothelial nitric oxide synthase, and transcription factors NF- κ B and AP-1. *Cardiovasc Res* 47:49–56.
- Verzola D, Bertolotto MB, Villaggio B, Ottonello L, Dallegri F, Frumento G, Berruti V, Gandolfo MT, Garibotto G, Deferran G. 2002. Taurine prevents apoptosis induced by high glucose in human tubule renal cells. *J Investig Med* 50:443–451.
- Zhang S, Bian Z, Gu C. et al. 2007. Preparation of anti-human cardiac troponin I immunomagnetic nanoparticles and biological activity assays. *Coll Surf B: Biointer* 55:143–148.
- Zhu H, Zhang C, Yin Y. 2005. Novel synthesis of copper nanoparticles: Influence of the synthesis conditions on the particle size. *Nanotechnology* 16:3079–3083.

Supplementary material available online

Supplementary Figure S1.